Segmentation methods for breast vasculature in dual-energy contrast-enhanced digital breast tomosynthesis

Kristen C. Lau, Hyo Min Lee, Tanushriya Singh, Andrew D. A. Maidment
{Kristen.Lau; Andrew.Maidment}@uphs.upenn.edu
University of Pennsylvania, Department of Radiology, 3400 Spruce Street, Philadelphia, PA 19104 USA

ABSTRACT

Dual-energy contrast-enhanced digital breast tomosynthesis (DE CE-DBT) uses an iodinated contrast agent to image the three-dimensional breast vasculature. The University of Pennsylvania has an ongoing DE CE-DBT clinical study in patients with known breast cancers. The breast is compressed continuously and imaged at four time points (1 pre-contrast; 3 post-contrast). DE images are obtained by a weighted logarithmic subtraction of the high-energy (HE) and low-energy (LE) image pairs. Temporal subtraction of the post-contrast DE images from the pre-contrast DE image is performed to analyze iodine uptake. Our previous work investigated image registration methods to correct for patient motion, enhancing the evaluation of vascular kinetics. In this project we investigate a segmentation algorithm which identifies blood vessels in the breast from our temporal DE subtraction images. Anisotropic diffusion filtering, Gabor filtering, and morphological filtering are used for the enhancement of vessel features. Vessel labeling methods are then used to distinguish vessel and background features successfully. Statistical and clinical evaluations of segmentation accuracy in DE-CBT images are ongoing.

Keywords: breast, contrast-enhanced, dual-energy, tomosynthesis, segmentation

1. INTRODUCTION

The observation that angiogenesis accompanies the formation of malignant breast lesions provides the motivation for contrast-enhanced (CE) imaging of the breast. The absorption of vascular contrast agents in malignant breast tissue is different than in normal breast tissue due to increased permeability in the new blood vessels. Thus, we can differentiate malignant breast tissue from benign tissue by observing the uptake of intravenous contrast agents.

The current gold standard for imaging breast cancer perfusion and vasculature is CE magnetic resonance imaging (MRI). CE-MRI is used as a screening method for high-risk women and for the characterization of lesions in the diagnosis of breast cancer. A gadolinium contrast agent is administered intravenously to highlight morphological features and vascular kinetics in CE-MRI. However, CE-MRI suffers from a trade-off between spatial and temporal resolution, and it does not visualize calcifications well, an early indication of breast cancer.

Digital breast tomosynthesis (DBT) is a FDA-approved breast imaging technique for acquiring high-resolution tomographic images at doses comparable to those used in mammography. An intravenous iodinated contrast agent is used to produce images of the breast vasculature in CE-DBT, which has the additional advantage of providing tomographic images of the morphology and three-dimensional (3D) localization of contrast-enhancing lesions. Furthermore, DBT has the ability to acquire functional characteristics of breast lesions at high spatial resolution, comparable (or even superior) to that of digital mammography.

Iodine uptake by breast tissue is made more evident by image subtraction. Overlapping anatomical structures that may otherwise occlude the detection and visualization of blood vessels are removed in image subtraction by suppressing variations in the anatomical signal. Dual-energy (DE) subtraction and temporal subtraction are two common types of image subtraction [1].

Low-energy (LE) and high-energy (HE) image pairs are acquired in DE imaging. Two distinct x-ray energies are used to differentiate the iodine signal from the soft tissue and to suppress the soft tissue signal. The x-ray energies are chosen so that the k-edge of the contrast agent lies within the range spanned by the LE and HE x-ray spectra. A weighted difference of the logarithms of the LE and HE images is used to create an iodine-enhancement image. Patient motion is minimized in DE subtraction because the HE and LE image pairs are acquired either simultaneously or rapidly in sequence.

Medical Imaging 2015: Physics of Medical Imaging, edited by Christoph Hoeschen, Despina Kontos,
Proc. of SPIE Vol. 9412, 941227 · © 2015 SPIE · CCC code: 1605-7422/15/$18 · doi: 10.1117/12.2081031

DE imaging, however, suffers from inherently lower sensitivity because the contrast-to-noise ratio is decreased when calculated as the difference of two energies.

Pre-contrast and post-injection images are acquired for temporal subtraction. An image of the iodine uptake is obtained via a logarithmic subtraction of the pre-contrast and post-contrast images. The subtraction results in the breast tissue signal being nulled. Temporal subtraction images are susceptible to patient motion artifacts because the total procedure time can be as long as 10 minutes. Although the breast is held in compression during the study, it is subject to involuntary motion arising from breathing as well as gross motion of the body over time. Additionally, we have observed that patients move as a reaction to the contrast injection. Consequently, there is a loss of lesion morphology and subtraction artifacts are formed, impeding the quantitative evaluation of iodine uptake.

In our previous work, we presented a hybrid subtraction method involving the temporal subtraction of the DE images. Image registration was employed to correct for patient motion during temporal subtraction. These innovations enhanced our ability to evaluate the vascular kinetics of breast tumors in CE-DBT imaging. We retain the high sensitivity of temporal subtraction while utilizing the resilience to motion of the DE technique [2].

Numerous anatomical studies of the breast have been conducted. However, there exist few comprehensive studies of the breast vasculature, and much of our knowledge of breast anatomy is based on the work of Sir Astley Cooper published in 1840 [3]. In addition to Cooper's work, investigative methods of mammary vasculature include the surgical dissection of specimens and radiography of the blood supply by Salmon in 1939 [4]. The arterial supply to the breast is derived primarily from branches of the internal thoracic artery, intercostal arteries, and the lateral thoracic artery. The venous anatomy of the breast parallels the arterial anatomy in the deep breast tissues, but it does not accompany the arterial supply superficially [5].

There is renewed interest in the study of breast anatomy, particularly that of the ductal and vascular systems, with the motivation to understand better the origins of breast cancer. We are interested in studying the breast vasculature because a better understanding of the vasculature network has many clinical implications, including the identification of thrombus, diagnosis of vascular masses, study of the symmetry of the vascularization of the breasts, and the detection, diagnosis, and removal of benign and malignant breast lesions. In addition, an improved knowledge of the breast vascular network would allow radiologists and surgeons to identify vascular anomalies important for surgical planning. Finally, a better understanding of the breast vasculature would allow us to develop and improve our 3D model of the breast. This would enhance the realism of software breast phantom simulations and aid in conducting virtual clinical trials.

A number of vessel segmentation methods have been developed for various anatomical structures in the body, including the liver and the eye. Hepatic vessel segmentation in computed tomography (CT) images is necessary for the 3D planning of liver surgery. The identification of the hepatic vessel network is necessary for the safe removal of tumors located near major blood vessels and in the surgical planning of oncological resections and living liver donations. It is also important to identify the hepatic vasculature network for the treatment planning of hepatic ablation procedures [6].

Segmentation methods have also been developed for the detection of small blood vessels in retinal images. Knowledge of the retinal vasculature is clinically important because abnormalities in these blood vessels are indicators of many diseases, including hypertension and diabetes. The detection of small vessels is difficult due to low contrast and tortuosity, and capillary vessels tend to have discontinuous flows [7].

We develop our method for breast vasculature segmentation by drawing inspiration from these segmentation methods and applications.

2. METHODS & MATERIALS

2.1 Image Acquisition

The University of Pennsylvania is conducting a CE-DBT clinical study in which patients with newly diagnosed breast cancers are imaged using a prototype DE Hologic Selenia Dimensions DBT system. The trial is IRB approved and is HIPAA compliant. The accrual goal is 100 patients and 10 patients have been imaged for the study to date. The goal of this study is to quantify the iodine uptake, as it is possible to exploit the linear relationship between the attenuation coefficient and the concentration of contrast agent. Another goal of the study is to compare CE-DBT to CE-MRI for concordance.

The Hologic prototype DE-DBT imaging system utilizes an x-ray source with a tungsten target. The system has an angular range of 15° and a single image acquisition lasts 7.3 seconds. A copper filter is used for the HE x-rays (49 kVp) and an aluminum filter is used for the LE x-rays (32 kVp). In order to accommodate breasts of different sizes, the mAs is varied to ensure adequate signal to the detector and an acceptable dose to the breast. 11 HE and 11 LE projections (total 22 projections) of the breast are acquired in an acquisition sequence. The LE and HE projection images are interleaved; this design allows the system to minimize patient motion within a single acquisition because the LE and HE images are obtained virtually simultaneously. Patients are seated and the breast is held in compression for the duration of the exam. The breast is imaged at four different time points (1 pre-contrast and 3 post-contrast). The unenhanced baseline image is obtained by acquiring a pre-contrast DE image set. A power injector is used to intravenously administer the iodinated contrast agent Visipaque-320 (GE Healthcare, Princeton, NJ) at 1 mL/kg to the patient. It is followed immediately by an intravenous saline flush. Three post-contrast images are acquired after injection: 20 seconds (arterial phase), 1 minute 25 seconds (venous phase), and 3 minutes 25 seconds (late phase). The timing of the post-injection images was determined from previous CE studies [8]. The image acquisition procedure is illustrated in Figure 1.

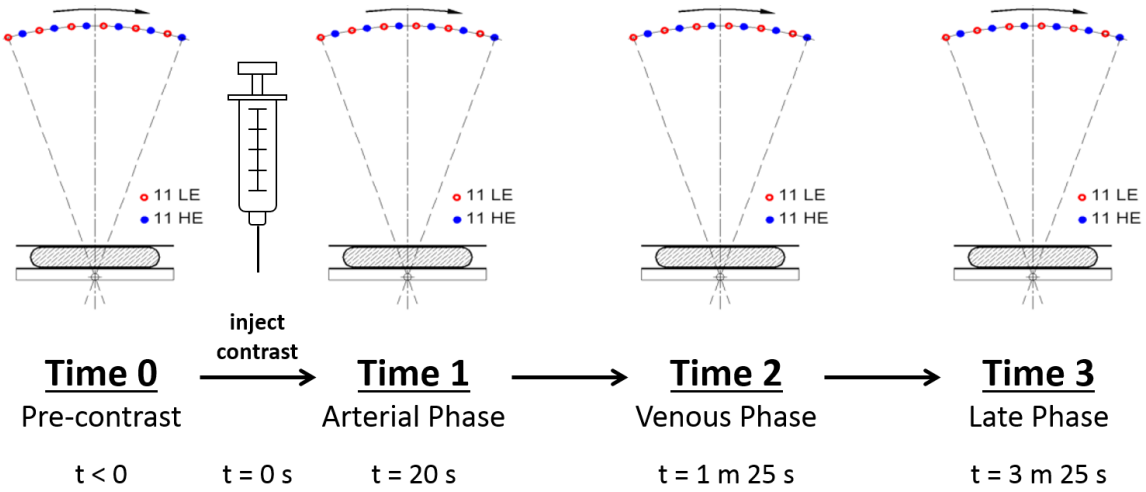

Figure 1. Illustration of the DE CE-DBT clinical trial imaging protocol.

2.2 Hybrid Image Subtraction

In our hybrid subtraction method, DE images are obtained at each time point via weighted logarithmic subtraction. The DE images are then temporally subtracted between the different time points to produce an iodine-enhanced image. The signal intensity *SI* of the DE image is expressed as a function of the HE and LE signal intensities:

$$SI^{DE} = SI^{HE} - w * SI^{LE} \tag{1}$$

where *w* is the DE weighting factor. The weighting factor *w* is calculated as

$$w = \frac{\mu_a^{HE} - \mu_g^{HE}}{\mu_a^{LE} - \mu_g^{LE}} = \frac{\ln(SI_a^{HE}) - \ln(SI_g^{HE})}{\ln(SI_a^{LE}) - \ln(SI_g^{LE})} \tag{2}$$

where μ is the linear attenuation coefficient and the superscripts a and g represent adipose tissue and glandular tissue, respectively. This is based on the work of Carton *et al.* [9]

Please refer to our previous paper [2] for additional details on the registration processes used in the hybrid image subtraction method.

2.3 Segmentation

2.3.1 Denoising

In this paper, we experiment with several edge-preserving denoising filters in order to enhance the performance of the segmentation algorithm. The median, bilateral, and anisotropic diffusion filters are considered.

The median filter is a non-linear denoising filter. The intensity value at each output pixel in the filtered image is replaced by the median value of the $m \times n$ region around the corresponding pixel in the input image.

The bilateral filter is a non-linear edge-preserving denoising filter. The intensity value at each output pixel is replaced by a weighted average of intensity values from pixels in a local neighborhood. It is similar to a Gaussian convolution, but it takes into account intensity variations for edge preservation. For an image *I*, the bilateral filter *BF* is given as

$$BF[I]_p = \frac{1}{W_p} \sum_{q \in S} G_{\sigma_s}(\|p - q\|) G_{\sigma_r}(I_p - I_q) I_q \tag{3}$$

and W_p is a normalization factor given by

$$W_p = \sum_{q \in S} G_{\sigma_s}(\|p - q\|) G_{\sigma_r}(I_p - I_q) \tag{4}$$

where G_{σ_s} is the spatial Gaussian kernel, G_{σ_r} is the range Gaussian kernel, σ_s is the spatial extent of a neighborhood, σ_r is the range parameter of an edge, and *p* and *q* denote two-dimensional (2D) pixel positions.

Our use of the anisotropic diffusion filter is based on the work of Keeling *et al*. [10].

2.3.2 Edge Enhancement

We implement an edge enhancement approach based on the multi-scale Gabor filter method for detecting retinal blood vessels developed by Rangayyan *et al*. [11], [12]. We propose to detect blood vessels in DBT images using Gabor filters to improve the efficiency of detection of thick and thin blood vessels. Gabor filters are directionally-selective bandpass filters that are often used to detect linear structures. They are sinusoidally-modulated Gaussian functions that have optimal localization in frequency and space domains. The kernel of the Gabor filter is given by:

$$G(x, y) = \frac{1}{2\pi\sigma_x\sigma_y} e^{-\frac{1}{2}\left(\frac{x'^2}{\sigma_x^2} + \frac{y'^2}{\sigma_y^2}\right)} \cos(2\pi f x') \tag{5}$$

where σ_x and σ_y are the standard deviations in the x and y directions, f is the frequency of the modulation sinusoid, $x' = x\cos\theta + y\sin\theta$, $y' = y\cos\theta - x\sin\theta$, and θ is the orientation angle. The parameters f, σ_x, and σ_y in equation (5) are adjusted to take into account the thickness of the blood vessels. Given τ is twice the thickness of the vessel and k is the elongation factor, the following relationship between the parameters is required to optimize our segmentation performance: $\sigma_x = \frac{\tau}{2\sqrt{2\ln 2}}$, $\sigma_y = k\sigma_x$, and $f = \frac{1}{\tau}$.

The described Gabor filter best detects linear features of positive contrast so that linear elements appear brighter than the background. The temporal DE images are convolved with Gabor kernels over many different orientations. The image features that match the features of the Gabor kernel produce maximal enhancement, whereas the background is comparatively unaffected.

Morphological filtering is then applied to the Gabor-filtered images to remove small geometric features in the background. Morphological operators are non-linear operators related to the shape features in an image. Morphological processing is constructed with operations on sets of pixels. They are dependent upon the relative ordering of pixel values, rather than individual numerical intensity values. Thus, they are well-suited for the processing of grayscale and binary images. Morphological filtering provides a tool for extracting image components that are useful in the representation and description of shapes in a region, such as boundaries.

2.3.3 Vessel Labeling

Although the Gabor filter enhances vessel edge features, it also enhances some background features. We use a threshold approach for vessel labeling. The simple threshold method assumes that the vessel voxel values are characterized by a higher intensity compared to the background voxels. Minimum and maximum threshold values for the breast vasculature are identified upon visual inspection. A summary of the segmentation process used in our investigation is summarized in Figure 2.

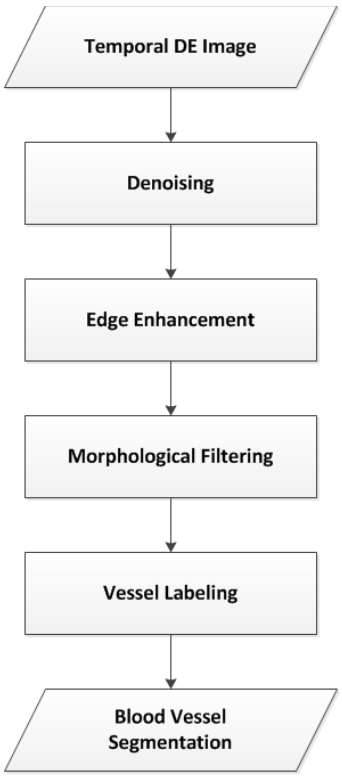

Figure 2. The segmentation method for identifying breast vasculature in DE CE-DBT.

3. RESULTS & DISCUSSION

3.1 Overview

In this paper, we present a 2D image segmentation method. This method is a slice-by-slice approach in which each 2D reconstructed image slice is registered individually. This procedure was applied to all 10 patients imaged in our study. A 3D image segmentation method designed to account for vessels that transition between image planes was not considered in this study.

3.2 Image Subtraction

In this paper, we present three clinical examples from our imaging study. A vertically-oriented blood vessel can be seen in Figure 3. A horizontally-oriented blood vessel can be seen in the patient shown in Figure 4. In the patient shown in Figure 5, we can see a horizontally-oriented blood vessel that branches in multiple directions. We choose to present these patients in this paper based on the characteristics of their vasculature network and to demonstrate the robustness of our segmentation method for vessels oriented in multiple directions.

3.3 Denoising

The median filter was found to smooth the entire image and vessel features were not preserved. Although the bilateral filter was edge-preserving, it also preserved some background features with sharp edges. The anisotropic diffusion filter performed the best because the vessel features are preserved well and the background features are sufficiently smoothed. A comparison of the filtering methods is summarized in Figure 6.

Patient #1

Figure 3. Temporal DE subtraction. The main blood vessel runs vertically.

Patient #2

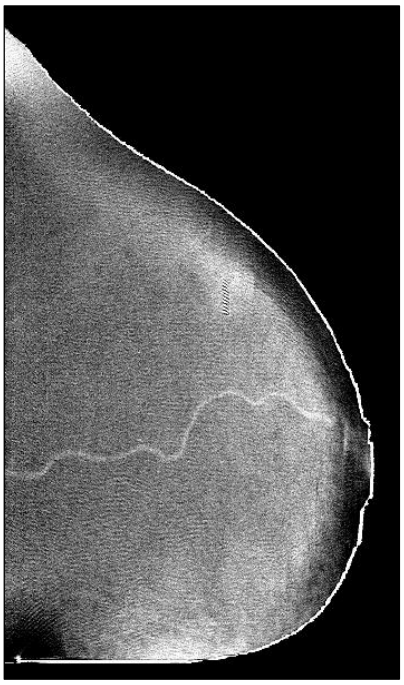

Figure 4. Temporal DE subtraction. The main blood vessel runs horizontally.

Patient #3

Figure 5. Temporal DE subtraction. The main blood vessel branches into multiple directions.

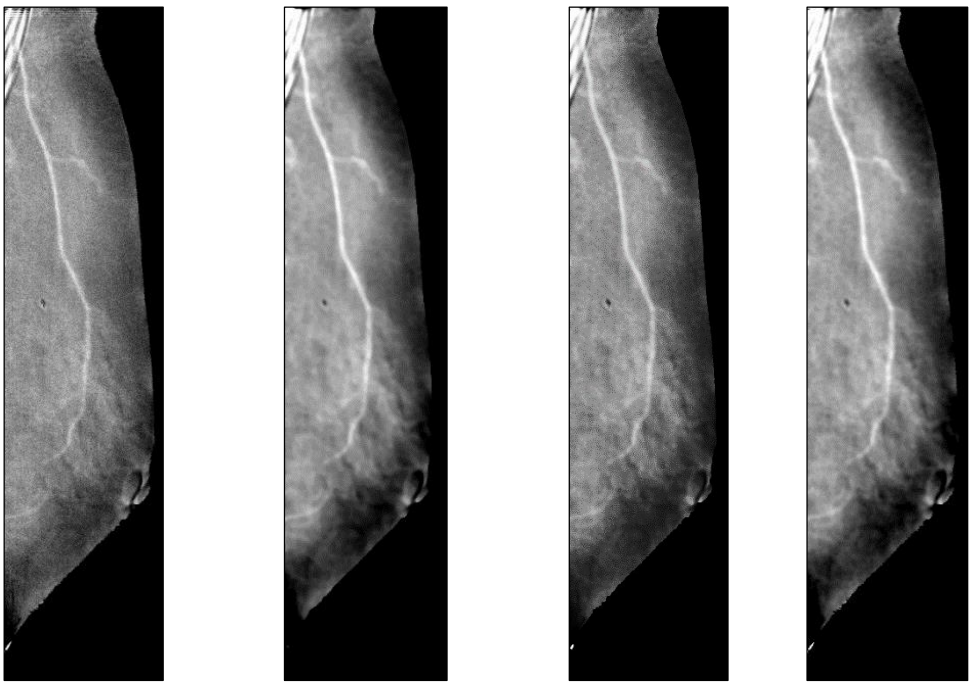

No Filter | Median Filter | Bilateral Filter | Anisotropic Diffusion Filter

Figure 6. Comparison of image filtering methods.

3.4 Edge Enhancement

Vessel enhancement using Gabor filters was performed for vessel segmentation. Our segmentation procedure demonstrates that the segmentation of blood vessels is resistant to directionality. The Gabor filter detects linear features of positive contrast so that linear elements appear brighter than the background. Figure 7 illustrates examples of our Gabor filtering results for the patients in our study. Magnified views of selected features in a particular 2D plane are shown.

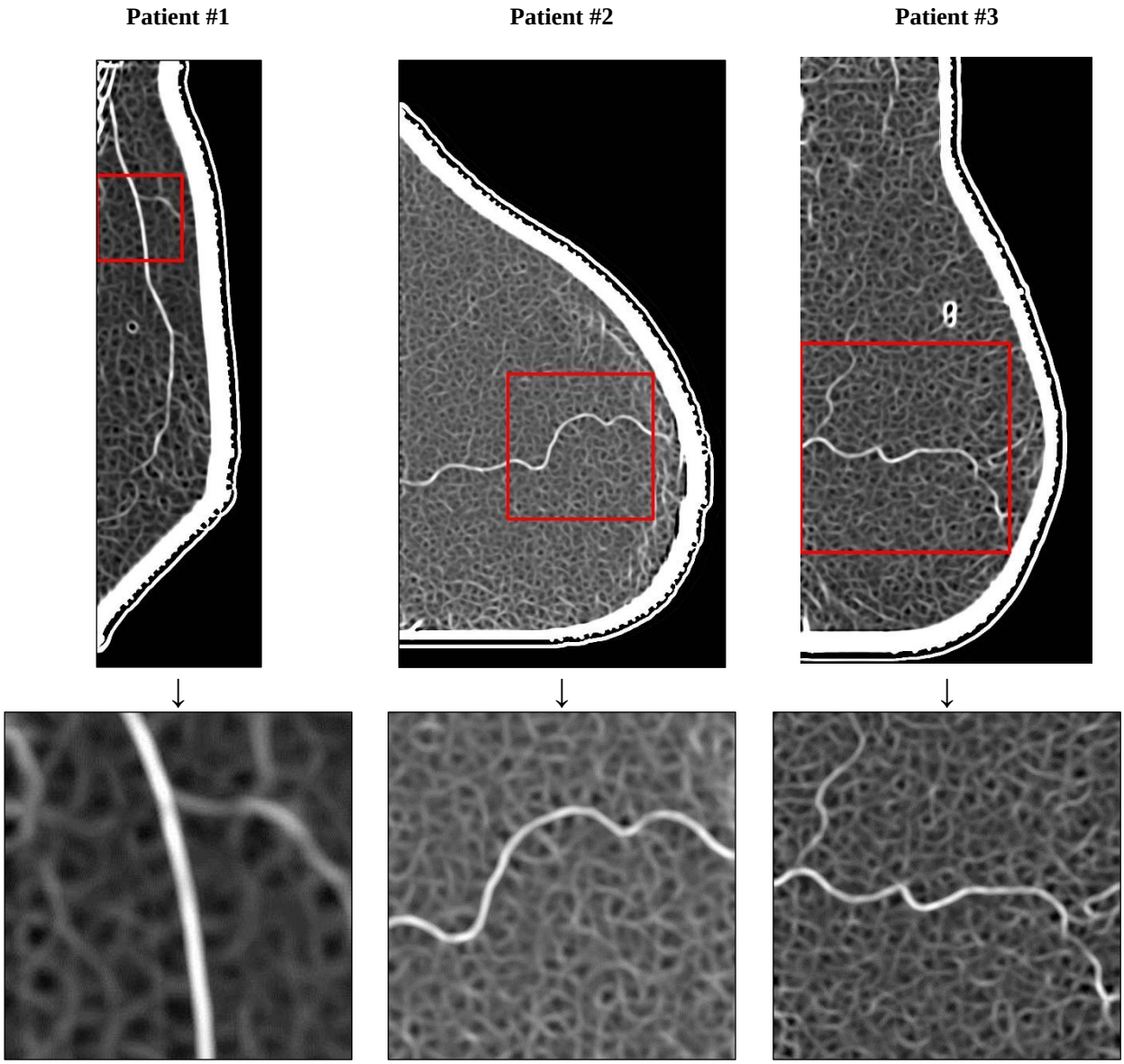

Figure 7. Summary of Gabor filter procedure for DE CE-DBT images.

We then applied morphological filtering to the Gabor-filtered images. Closing and erosion filters were used. Figure 8 illustrates examples of our morphological filtering results applied to the Gabor-filtered images. Similarly, magnified views of selected features in a particular 2D plane are shown.

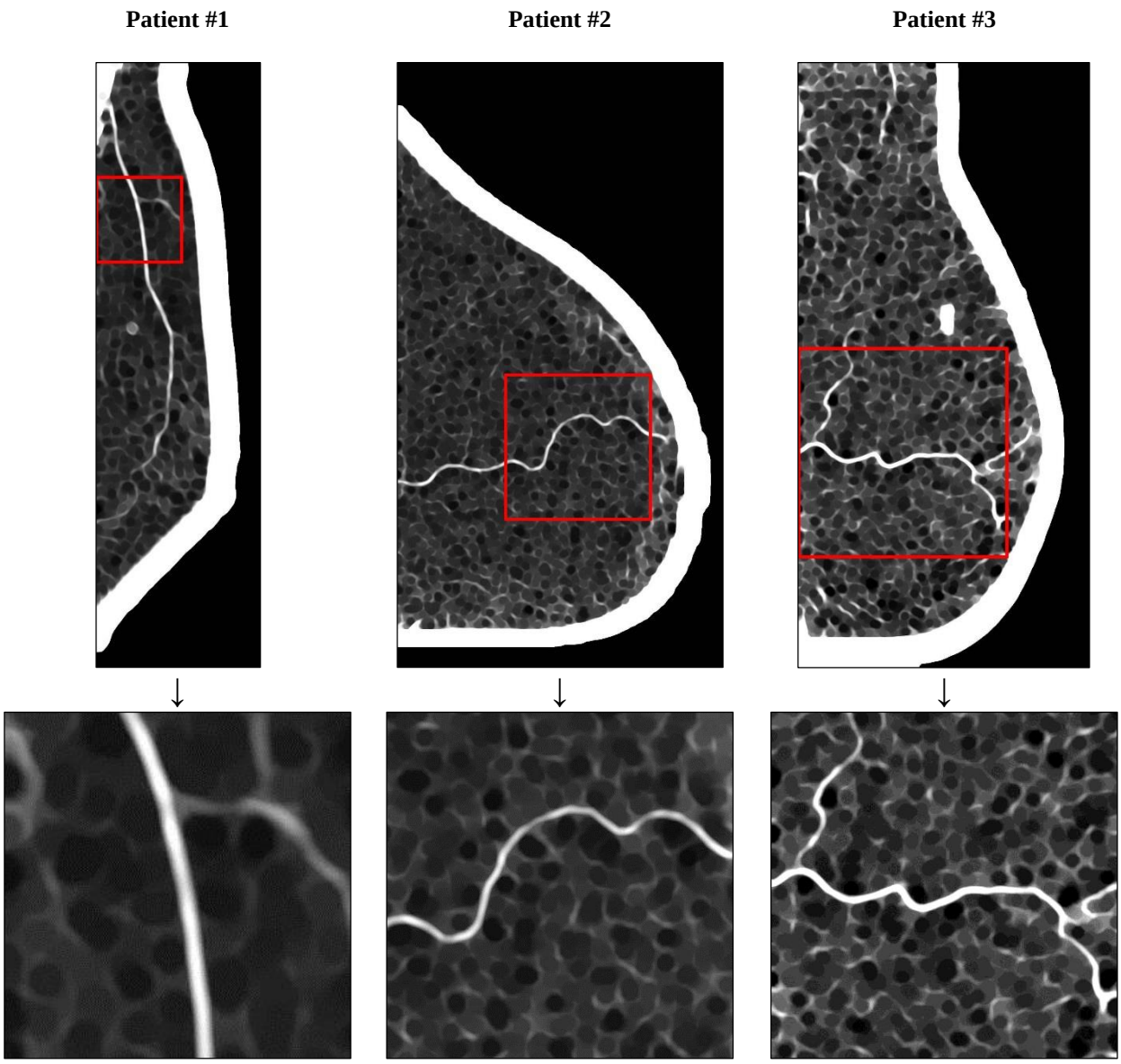

Figure 8. Summary of morphological filtering procedure.

Upon close inspection, we show that the small branch-like and circular geometric shapes in the background of the Gabor-filtered images are removed after morphological filtering. The contrast between the vessel and background tissue is increased.

3.5 Vessel Labeling

A preliminary, feature based, clinical evaluation of our segmentation results was conducted. In order to label the vessels with high specificity, a simple threshold was performed. This method removed much of the background features, while labeling the vessels accurately. The threshold method provides reasonable vessel labeling at low computational costs. A limitation of this method is that it may incorrectly label false-enhancements, making the interpretation of results unreliable. To determine the robustness of the segmentation algorithm, we examine the segmentation of blood vessels oriented in multiple directions.

We present in Figure 9 an example of a patient with a small sized breast. The segmented blood vessel is shown in the red overlay. It can be seen that the main blood vessel runs vertically in the direction of motion of the x-ray tube. This blood vessel is strongly visible in each of the reconstructed slices, and it is known that DBT has poor slice resolution for objects with a vertical orientation.

In comparison, Figure 10 is an example of a patient with a larger breast. The segmented blood vessel is shown in the red overlay. The main blood vessel is oriented horizontally, and it is known that sensitivity to motion is greatest in the horizontal direction in DBT. These results indicate that the segmentation algorithm can successfully segment blood vessels that are oriented in multiple directions.

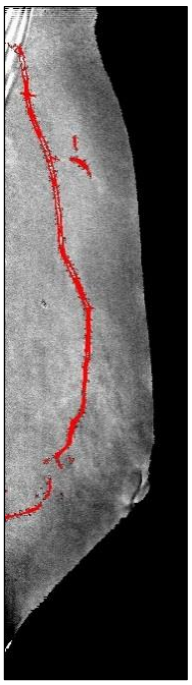

Figure 9

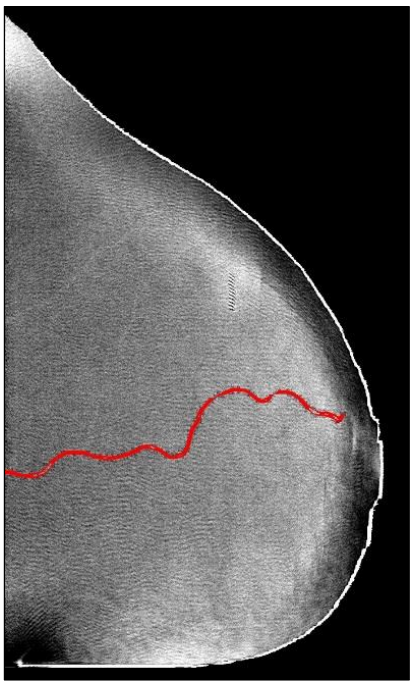

Figure 10

Our segmentation procedure demonstrates that the segmentation of blood vessels is resistant to directionality. The object boundaries are well-defined and the vessels appear continuous when they are completely visible within a plane of the breast. However, a limitation of our segmentation approach is that it depends upon the patient's iodine uptake and the success of our registration and subtraction methods. Poor contrast agent uptake could result in poor registration results and object visualization. Consequently, the identification of blood vessels in temporal DE images would be impeded in the segmentation process. As a further development in our analysis, it would be beneficial to investigate alternate vessel labeling methods, such as binary graph cut methods. In addition, it would be advantageous to consider a 3D approach to vessel segmentation using vessel tracking methods.

3.6 Quantitative Evaluation

In order to evaluate the success of our blood vessel segmentations, we compared the automated segmentation with ground truth manual segmentation. The ground truth segmentation was provided by a trained specialist. Vessel structures were identified and contoured using the ITK-SNAP software [13]. In this current paper, we evaluate segmentation accuracy based upon the following statistical measures that compare the similarity between two samples: Dice similarity coefficient, false positive rate, and false negative rate. These statistical measures can be expressed mathematically as

$$\text{Dice Similarity Coefficient:} \quad \frac{2(M_V \cap A_V)}{M_V + A_V} \tag{6}$$

False Positive Rate (FPR): $$\frac{2(M_T \cap A_V)}{M_V + A_V} \quad (7)$$

False Negative Rate (FNR): $$\frac{2(M_V \cap A_T)}{M_V + A_V} \quad (8)$$

where *M* represents the manual segmentation, *A* represents the automatic segmentation method, *T* represents tissue class pixels, and *V* represents vessel class pixels. For example, M_V represents the number of vessel pixels identified using the manual segmentation method.

We use the Dice similarity coefficient (DSC) as a statistical validation metric to evaluate the spatial overlap accuracy of our automated segmentation algorithm for DE CE-DBT images, illustrated in three clinical examples. A DSC value of 1 indicates perfect agreement between the two segmentation sets and a DSC value of 0 indicates there is no overlap between the two sets. In image segmentation, a larger DSC value would indicate that the automated results match the ground truth better than results that have lower DSC values. A false positive represents an erroneous labeling in which the presence of a blood vessel is improperly indicated. The false positive rate represents the rate of occurrence of vessel pixels in an image that are known to be tissue pixels. Conversely, a false negative represents the case in which a blood vessel is not identified when in reality it is present.

Table 1. Summary of quantitative evaluation of segmentation method.

Patient	DSC	FNR	FPR
1	0.526	0.061	0.310
2	0.577	0.024	0.541
3	0.569	0.022	0.526
Average	0.557	0.036	0.459

We observe satisfactory validation results for the three clinical examples, and the average DSC value is 0.557. An average false negative rate of 0.036 indicates that our segmentation method successfully identifies vessels when they are present. The results for the three clinical examples presented in this paper are summarized in Table 1.

4. FUTURE WORK

Our imaging study is limited by the number of patients recruited for the study. We have only been able to image 10 women to date and subject recruitment for our study is ongoing. Further investigation of this study involves investigating alternative methods for segmentation, such as binary graph-cut methods for vessel labeling. The binary graph-cut method is a statistical segmentation approach that identifies each voxel in the image as a blood vessel or background tissue. This method determines a minimum cost cut that divides the image into the two classes. A useful advantage of applying the graph-cut method is that the cut can be regularized to be smoother. Training dataset is provided with manually segmented vessel-enhancements for "vessel class" and background voxels including false-enhancements for "non-vessel class".

Vessel tracking can be explored as a 3D approach for vessel segmentation in DE CE-DBT images. Vessel tracking has the advantage of guaranteeing the connectedness of vessel segments, and it would allow for better quantitative analysis of the vasculature than possible using pixel classification methods. Intrinsic geometrical and topographical information is provided using vessel tracking methods, including vessel width, curvature, and length. By identifying the blood vessels in the breast, we can use the segmentation to create a 3D model of breast vasculature and incorporate the vascular tree into a 3D model of the breast. Finally, image evaluation by trained radiologists will provide us with insight on the diagnostic feasibility of DE CE-DBT.

5. CONCLUSION

In our study, we successfully developed breast vasculature segmentation methods for DE CE-DBT images. An approach involving anisotropic diffusion filtering and Gabor filtering provided successful edge enhancement results. In addition, vessel labeling using a threshold method was able to remove false-enhancement features in the background and

retained the true vessel labels. However, a number of false-positive pixels were observed and we are currently investigating methods to address this issue.

We have illustrated a statistical validation analysis of spatial overlap using manual and automated vessel segmentations in three clinical examples. Using our current segmentation schema, we can achieve 56% accuracy with our clinical examples, as described by the DSC value. The DSC value is a simple and useful summary measure of spatial overlap accuracy.

Methods for the detection and quantitative analysis of the vascular architecture in the breast have the potential to aid in the detection and diagnosis of breast cancers. An ultimate goal of the study is the quantitative evaluation of the iodine uptake in the breast. Further investigation involves using our segmentation method to create a 3D model of the breast vasculature. This will be compared with a calibration vessel phantom to determine total iodine uptake in the breast. As clinical and research interests in breast vascularity continue to evolve, we can use these segmentation methods to develop quantitative techniques for longitudinal clinical analysis, including: clinical follow-up of patients, analysis of the progression of disease, evaluation of treatment efficacy, and design of better treatment protocols.

ACKNOWLEDGMENTS

The project described is supported in part by Grant Number UL1RR024134 from the National Center for Research Resources. The content is solely the responsibility of the authors and does not necessarily represent the official views of the National Center for Research Resources or the National Institutes of Health. This work is also supported in part by the Institute for Translational Medicine and Therapeutics' (ITMAT) Transdisciplinary Program in Translational Medicine and Therapeutics. The prototype imaging system is provided to Penn by Hologic (Bedford, MA) under a research agreement. The authors wish to acknowledge the assistance of Jing Zhenxue, Andy Smith, Barry Ren and Chris Ruth from Hologic for technical assistance. The authors would also like to thank Paul Yushkevich for many helpful conversations.

REFERENCES

[1] A.K. Carton, S. C. Gavenonis, J. A. Currivan, E. F. Conant, M. D. Schnall, and A. D. A. Maidment, "Dual-energy contrast-enhanced digital breast tomosynthesis - a feasibility study.," *Br. J. Radiol.* **83**(988), 344–350 (2010) [doi:10.1259/bjr/80279516].

[2] K. C. Lau, S. Roth, and A. D. A. Maidment, "2D and 3D registration methods for dual-energy contrast-enhanced digital breast tomosynthesis," *Proc. SPIE 9033, Med. Imaging 2014 Phys. Med. Imaging* **9033**, 90335W – 1–90335W – 11 (2014) [doi:10.1117/12.2044080].

[3] A. P. Cooper, "On the anatomy of the breast, volume I," *Anat. breast, by Sir Astley Past. Cooper* (1840).

[4] L. Cunningham, "The Anatomy of the Arteries and Veins of the Breast," *J. Surg. Oncol.* **9**(1), 71–85 (1977).

[5] R. A. Jesinger, G. E. Lattin, E. A. Ballard, S. M. Zelasko, and L. M. Glassman, "Vascular Abnormalities of the Breast: Arterial and Venous Disorders, Vascular Masses, and Mimic Lesions with Radiologic-Pathologic Correlation," *Radiographics* **31**(7), E117–E136 (2011) [doi:10.1148/rg.317115503].

[6] J. N. Kaftan, H. Tek, and T. Aach, "A two-stage approach for fully automatic segmentation of venous vascular structures in liver CT images," *Proc. SPIE 7259, Med. Imaging 2009 Image Process.*, 725911–725911 – 12 (2009) [doi:10.1117/12.812407].

[7] J. V. B. Soares, J. J. G. Leandro, R. M. Cesar Júnior, H. F. Jelinek, and M. J. Cree, "Retinal vessel segmentation using the 2-D Gabor wavelet and supervised classification.," *IEEE Trans. Med. Imaging* **25**(9), 1214–1222 (2006) [doi:10.1109/TMI.2006.879967].

[8] S. Gavenonis, K. Lau, R. Karunamuni, Y. Zhang, B. Ren, C. Ruth, and A. D. A. Maidment, "Initial Experience with Dual-Energy Contrast-Enhanced Digital Breast Tomosynthesis in the Characterization," *Breast Imaging SE - 5* **7361**, A. D. A. Maidment, P. Bakic, and S. Gavenonis, Eds., 32–39, Springer Berlin Heidelberg (2012) [doi:10.1007/978-3-642-31271-7_5].

[9] A.K. Carton, C. Ullberg, K. Lindman, R. Acciavatti, T. Francke, and A. D. A. Maidment, "Optimization of a dual-energy contrast-enhanced technique for a photon-counting digital breast tomosynthesis system: I. A theoretical model," *Med. Phys.* **37**(11), 5896 (2010) [doi:10.1118/1.3490556].

[10] S. L. Keeling and R. Stollberger, "Nonlinear anisotropic diffusion filtering for multiscale edge enhancement," *Inverse Probl.* **18**(1), 175–190 (2002) [doi:10.1088/0266-5611/18/1/312].

[11] R. M. Rangayyan, "Detection of blood vessels in the retina with multiscale Gabor filters," *J. Electron. Imaging* **17**(2), 023018 (2008) [doi:10.1117/1.2907209].

[12] R. M. Rangayyan and F. J. Ayres, "Gabor filters and phase portraits for the detection of architectural distortion in mammograms," *Med. Biol. Eng. Comput.* **44**(10), 883–894 (2006) [doi:10.1007/s11517-006-0088-3].

[13] P. A. Yushkevich, J. Piven, H. C. Hazlett, R. G. Smith, S. Ho, J. C. Gee, and G. Gerig, "User-guided 3D active contour segmentation of anatomical structures: Significantly improved efficiency and reliability," *Neuroimage* **31**(3), 1116–1128 (2006) [doi:10.1016/j.neuroimage.2006.01.015].